Journal of Inflammation Research

Dovepress
Taylor & Francis Group

Open Access Full Text Article

ORIGINAL RESEARCH

Acupotomy Alleviates Capsular Fibrosis in Frozen Shoulder Rats by Modulating CCL2 to Inhibit Macrophage Recruitment and Suppress the Inflammatory Response

Hao Liang[1], Jialin Li[1], Su Qiu[1], Jinyuan Guo[1], Jianmin Liu[1–3]

[1]College of Acupuncture-Moxibustion and Orthopedics, Hubei University of Chinese Medicine, Wuhan, Hubei, People's Republic of China; [2]Hubei Shizhen Laboratory, Hubei University of Chinese Medicine, Wuhan, Hubei, People's Republic of China; [3]Hubei Provincial Collaborative Innovation Center of Preventive Treatment by Acupuncture and Moxibustion, Hubei University of Chinese Medicine, Wuhan, Hubei, People's Republic of China

Correspondence: Jianmin Liu, College of Acupuncture-Moxibustion and Orthopedics, Hubei University of Chinese Medicine, Wuhan, Hubei, People's Republic of China, Email 1356@hbucm.edu.cn

Background: Frozen shoulder (FS) is a debilitating condition characterized by chronic inflammation and fibrosis of the glenohumeral capsule. Macrophage recruitment, facilitated by C-C motif chemokine ligand 2 (CCL2), plays a crucial role in tissue fibrosis progression. Acupotomy has proven effective in alleviating FS symptoms; however, the mechanism by which it influences CCL2-mediated macrophage chemotaxis in FS requires further exploration.

Methods: Forty male Sprague-Dawley rats were randomly assigned to four groups (n = 10 per group): Control (no modeling/intervention), Untreated (FS modeling only), Acupotomy (FS model + acupotomy therapy), and Sham Apo (FS model + superficial acupotomy stimulation). FS was induced by unilateral shoulder plaster immobilization. The Acupotomy and Sham Apo groups then underwent their respective procedures (once weekly; two sessions in total). Shoulder function was evaluated using arthritis scoring, gait analysis, and maximum passive abduction angle measurement. Pathological changes were examined using hematoxylin and eosin and Masson's trichrome staining. Inflammation- and fibrosis-related molecules in serum and tissue samples were detected using biochemical and molecular biology analyses. Macrophage-related biomarkers, CCL2, and α-SMA were evaluated by immunostaining, with protein-protein docking for further analysis.

Results: Acupotomy significantly enhanced shoulder function and mobility in FS rats. Histopathological analysis revealed that the capsular structure improved after acupotomy with notably decreased inflammatory infiltration and collagen deposition. Furthermore, acupotomy markedly reduced inflammation- and fibrosis-related factors in both serum and lesion tissues. Mechanistic studies demonstrated that acupotomy diminished macrophage recruitment, adjusted the M1/M2 polarization ratio, and reduced α-SMA expression, all of which were linked to CCL2 inhibition. Further analysis confirmed a positive correlation between CCL2 and α-SMA expression, and protein-protein docking suggested potential interactions between CCL2 and macrophage polarization markers and α-SMA.

Conclusion: Acupotomy demonstrated significant efficacy in enhancing shoulder function and reducing fibrosis in FS rats, primarily by suppressing inflammatory responses and inhibiting CCL2-mediated macrophage recruitment.

Keywords: acupotomy, frozen shoulder, macrophages, CCL2, fibrosis

Introduction

Frozen shoulder (FS), also known as adhesive capsulitis, is a chronic condition characterized by shoulder pain and a gradual decline in function.[1,2] It affects 2–5% of the general population, often leading to significant limitations in daily activities and negatively impacting quality of life.[1] Current clinical management primarily includes physical therapy and intra-articular steroid injections.[3] While these interventions may relieve pain, they have shown limited effectiveness in

Received: 28 June 2025
Accepted: 14 November 2025
Published: 21 November 2025

Graphical Abstract

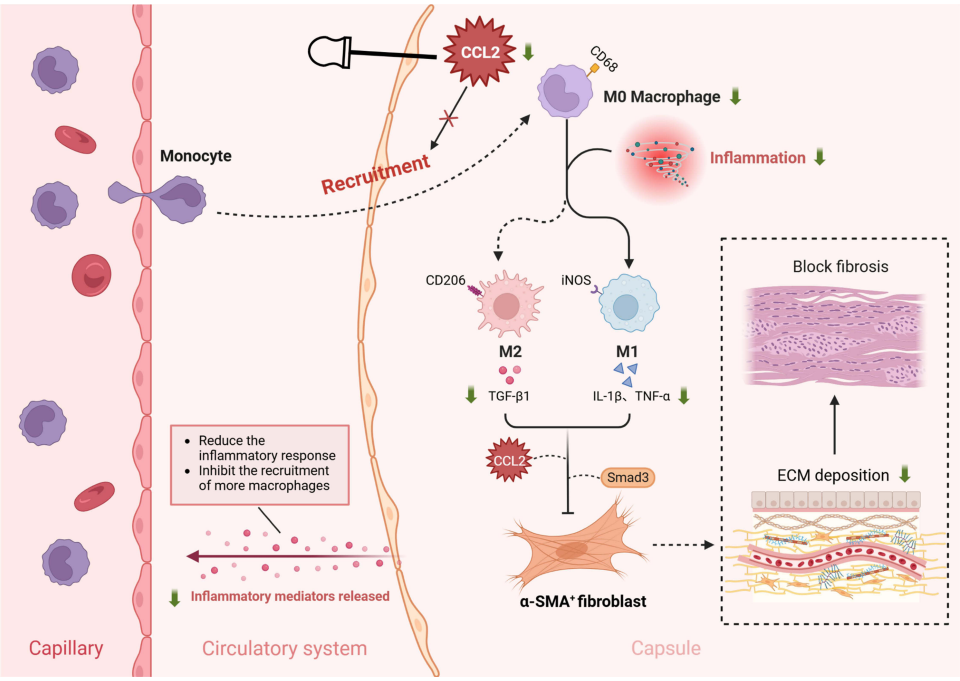

improving shoulder function, do not address the underlying pathological mechanisms, and have drawbacks such as delayed onset and dosage dependence.[4,5] Consequently, standardized treatments still encounter numerous challenges.

Current research indicates that FS is a dynamic process characterized by chronic inflammation and fibrosis.[6,7] Persistent inflammation recruits and activates immune cells, prompting them to release growth factors, chemokines, and proinflammatory mediators, thereby amplifying the inflammatory response and accelerating fibrosis.[8] Macrophages are pivotal to this process. The recruitment of macrophages to inflamed areas serves as an initiating factor for fibrosis, and macrophage polarization triggered by inflammatory signals directly influences fibrogenesis.[9,10] Specifically, M1 macrophages extend the inflammatory cycle by releasing pro-inflammatory factors such as tumor necrosis factor (TNF)-α and interleukin (IL)-1β, which exacerbate tissue damage and consequently induce fibrotic formation.[11] Conversely, M2 macrophages produce substantial amounts of growth factors, such as transforming growth factor (TGF)-β1, which activate fibroblasts and exacerbate fibrosis by promoting excessive extracellular matrix (ECM) deposition.[12,13] Chemokine (C-C motif) ligand 2 (CCL2) is a critical inflammatory mediator that influences monocyte/macrophage chemotaxis and activity.[14] It regulates inflammatory immunity and tissue remodeling by recruiting macrophages to damaged tissues, which plays a significant role as a driving force in the fibrotic process.[15,16] As documented in a previous study, the administration of CCL2 antagonist pCAGGS-7ND to osteoarthritic rats significantly reduced macrophage infiltration and fibrotic area in the infrapatellar fat pad.[17] Thus, inhibiting the aberrant recruitment of macrophages by CCL2 is anticipated to be a potentially effective therapy for FS.

Acupotomy, a minimally invasive intervention that integrates the features of both the “filiform needle” and the “scalpel”, effectively enhances local blood circulation and facilitates the self-repair of soft tissues through the precise release of adhesions at the affected region, thereby restoring local microenvironment homeostasis.[18] Studies have confirmed that acupotomy can reduce inflammation and increase shoulder mobility effectively, and guidelines recommend it as a reliable therapy for FS.[19,20] Although acupotomy is widely used clinically to alleviate FS symptoms, the specific mechanism by which it mitigates inflammatory fibrosis of the glenohumeral capsule remains unclear.

This study aimed to examine the therapeutic effects and underlying mechanisms of acupotomy in FS. We established an FS model by immobilizing the unilateral shoulder of rats using plaster for 21 days. Our approach involved a systematic evaluation of the impact of acupotomy on shoulder function and capsular fibrosis, alongside an investigation into its mechanism of action in FS treatment through the recruitment of macrophages mediated by CCL2 and the modulation of macrophage polarization. This study may provide new insights into the role and mechanism of acupotomy in addressing FS.

Materials and Methods

Experimental Protocol and Frozen Shoulder Modeling

All animal experiments were performed at Hubei Provincial Center for Disease Control and Prevention and were approved by its Institutional Animal Care and Use Committee (Approval No. 202420084). All procedures were conducted in accordance with the Guide for the Care and Use of Laboratory Animals. The experimental animals were purchased from SCBS Bio-Technology Co. Ltd (Henan, China; License No. SCXK 2020-0005). Forty male Sprague-Dawley rats (9-week-old, 350–400 g) were kept under SPF conditions (12-hour light/dark cycle, 20–24°C, and 40–60% humidity) with unlimited access to food and water, and were randomly divided into Control, Untreated, Acupotomy, and Sham Apo groups (n = 10 per group). The Control group received no modeling or intervention. The Untreated group underwent FS modeling without intervention. Both the Acupotomy and Sham Apo groups received acupotomy intervention once per week for two consecutive weeks after FS modeling, targeting identical anatomical sites but using different procedural approaches. After acclimatization, rats in the Untreated, Acupotomy, and Sham Apo groups were anesthetized with isoflurane inhalation (3–4% induction, 2–2.5% maintenance). Their left glenohumeral joint and forelimb were then immobilized in an internal rotation position against the anterior thorax using unilateral shoulder casts for 21 days.[21,22] (Figure 1A). Plaster-immobilized rats required daily observation and re-fixing if loosened.

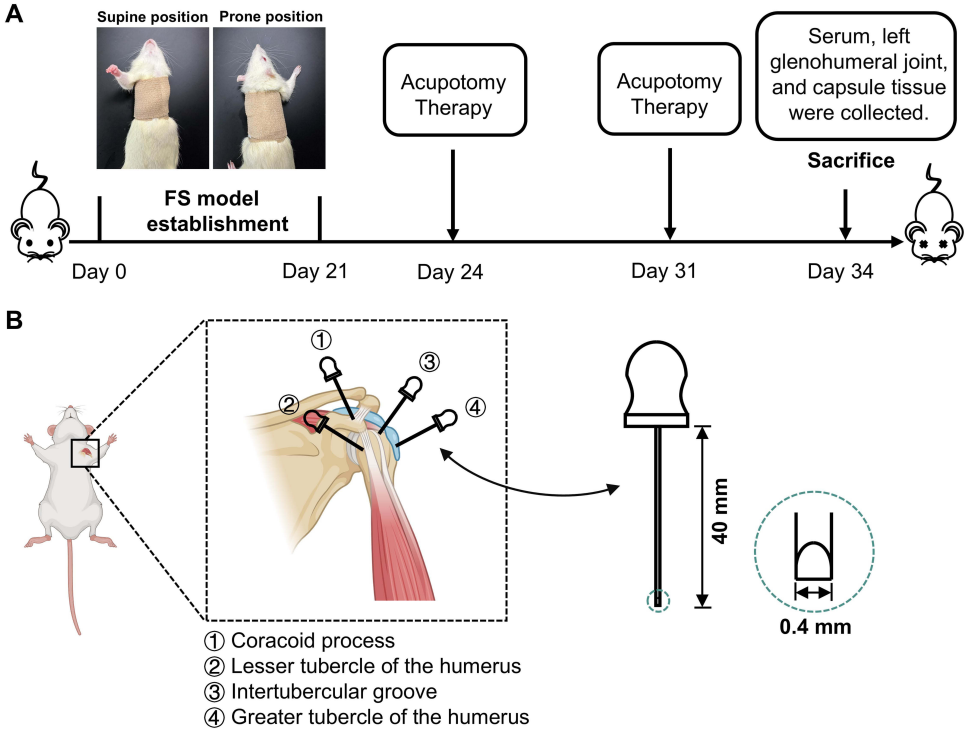

Figure 1 Experimental procedure and treatment protocol. (**A**) Experimental flowchart. The upper section presents representative images of the rat positioned in both supine and prone orientations following plaster immobilization. (**B**) Acupotomy intervention locations and detailed specifications of acupotomy instrument. Some graphical assets were created on *BioRender*. Liang, H. (2025) https://BioRender.com/iop6jdb.
Abbreviation: FS, frozen shoulder.

https://doi.org/10.2147/JIR.S550202

Procedure for Acupotomy

Under isoflurane anesthesia, the rats were positioned supine, and the left shoulder was shaved. The coracoid process, lesser and greater tubercles of the humerus, and intertubercular groove were all marked. Following skin sterilization, treatment was administered using 0.4×40 mm acupotomy needles (Huayou Medical Devices Co., Ltd. Jiangsu, China).[20,23] (Figure 1B) The anatomical structures and operating procedures are presented in Table S1. After the needles were discharged, a sterile cotton ball was pressed onto the punctum for 1 min to prevent bleeding, followed by sterilization. In the Sham Apo group, needles were inserted superficially without performing a release procedure, with subsequent management matching that of the Acupotomy group. The Control and Untreated groups received no treatment. Acupotomy was performed once a week for a total of two sessions. The sites were sterilized daily and observed for 3 days post-procedure. Two licensed Chinese medical practitioners performed the acupotomy independently to ensure reproducibility of the procedure.

Shoulder Inflammation Assessment

Based on the arthritis scoring method described by Honzawa et al,[24] scores of 0–3 were assigned to assess erythema, shoulder swelling, joint stiffness of the affected left forelimb, and shoulder stiffness to evaluate the improvement in shoulder inflammation following acupotomy. Score 0, no erythema, shoulder swelling, or joint stiffness; score 1, mild erythema and shoulder swelling; score 2, marked erythema and shoulder swelling; and score 3, severe erythema, shoulder swelling, and joint stiffness. All 10 rats in each group were subjected to this evaluation. The scoring was performed independently by two experimenters.

Gait Analysis

We made a gait analysis device based on voluntary walking by referring to the method of Min et al.[25] In each group, all 10 rats had their forepaws separately coated with red (left forepaws) and blue (right forepaws) non-toxic dyes, and were then placed in the starting box, generating colored paw prints along the passageway during traversal. The area of the prints was quantified using ImageJ software (National Institutes of Health, MD, USA) to assess the joint endurance, providing insights into shoulder function.[26] To calculate the more accurate area, three consecutive paw prints were collected from both sides and averaged for statistical analysis. Data from incorrect walking patterns were discarded, and the procedure was repeated two to three times to obtain the consecutive prints.

Measurement of Maximum Passive Abduction Angle

Referring to the method of Qiao et al,[27] the intact left (affected) scapula and proximal two-thirds of the humeral stem with the associated muscle tissue were excised during sampling. A syringe needle (1.2 cm × 0.45 mm) was inserted into the humeral stem with a surgical suture attached to the tail. Two identical syringe needles were vertically inserted into the upper and lower corners of the scapula and secured to a foam plate. The surgical suture was attached to a transverse tensiometer with a 5 N constant tensile force applied to the humeral stem. The angle between the inferior angle of the scapula and humeral stem was measured using a goniometer for maximal passive abduction. Three measurements were taken and averaged for statistical analysis. The target shoulders of 10 rats in each group were subjected to this measurement. The procedure was completed within 15 min to prevent tissue damage.

Enzyme-Linked Immunosorbent Assay (ELISA)

Five serum samples per group were assayed according to the protocol of the ELISA kit (R&D Systems, IL-1β: VAL903; TNF-α: VAL903; TGF-β1: DB100C), and the absorbance values of the samples were measured using an enzyme labeling instrument (iMark-1681130, Bio-Rad, California, USA) set at 450 nm as the detection wavelength and 630 nm as the correction wavelength. The concentrations of IL-1β, TNF-α, and TGF-β1 in the serum were calculated by comparison with the standards.

Table 1 Primer Sequences for RT-qPCR

Target Gene	Primer Sequence (5′-3′)	Product Length
Il1b	Forward: 5′-GCTTCAAATCTCACAGCAGCAT-3′ Reverse: 5′-TAGCAGGTCGTCATCATCCCAC-3′	196
Tnfα	Forward: 5′-CCGATTTGCCATTTCATACCAG-3′ Reverse: 5′-TCACAGAGCAATGACTCCAAAG-3′	232
Ifng	Forward: 5′-GTTTTGCAGCTCTGCCTCAT-3′ Reverse: 5′-CGTCCTTTTGCCAGTTCCTC-3′	160
Tgfβ1	Forward: 5′-GAAGGACCTGGGTTGGAAGT-3′ Reverse: 5′-CGGGTTGTGTTGGTTGTAGA-3′	136
Smad3	Forward: 5′-CAGCGAGTTGGGGAGACATT-3′ Reverse: 5′-CCTGGGGGTATCTTGCAGAC-3′	287
Col1a1	Forward: 5′-TTCACCTACAGCACGCTT-3′ Reverse: 5′-ATGTCCATTCCGAATTCC-3′	158
Gapdh	Forward: 5′-ACAGCAACAGGGTGGTGGAC-3′ Reverse: 5′-TTTGAGGGTGCAGCGAACTT-3′	254

Reverse Transcription-Quantitative Polymerase Chain Reaction (RT-qPCR)

Five capsule tissue samples were obtained from the left (affected) glenohumeral joint in each group for RT-qPCR analysis. Each sample was individually homogenized using TRIzol reagent (R401-01, VAZYME) to extract total RNA. Complementary DNA (cDNA) was synthesized from the extracted RNA via reverse transcription using a cDNA synthesis kit (R223-01, VAZYME). The primer sequences for *Il1b, Tnfα, Ifng, Tgfβ1, Smad3*, and *Col1a1* were obtained from the publicly accessible NCBI database (National Institutes of Health, MD, USA) and are listed in Table 1. The PCR system comprised 4 μL of diluted cDNA in a total volume of 20 μL. Gene expression was quantified using a QuantStudio 6 Real-Time PCR System. The PCR conditions were as follows: 95°C for 10 min; 95°C for 15s, 60°C for 60s, for a total of 40 cycles. Target gene expression was determined using the $2^{-\Delta\Delta Ct}$ method, with *Gapdh* as an internal reference.

Histopathological Evaluation

Five shoulders were randomly selected from the left (affected) side in each group for histological and immunostaining analysis. Following fixation in paraformaldehyde, decalcification, and paraffin embedding, the samples were sectioned into consecutive 5 μm-thick slices for subsequent hematoxylin and eosin (H&E) staining, Masson's trichrome staining, immunohistochemistry, and immunofluorescence. For all staining procedures, each specimen was processed on a continuous slice basis to ensure histological evaluation of comparable tissue regions.

H&E and Masson's trichrome staining were used for histopathological assessment. Specifically, H&E staining was used for histological analysis, and Masson's trichrome staining was used to evaluate the degree of collagen deposition. Tissue morphology was examined using a white-light microscope (CX31, Olympus, Tokyo, Japan) and photographed. Three random areas from each section were photographed and scored for synovial cell layer hyperplasia, cell density, and inflammatory infiltration.[28] The scoring criteria are provided in Table S2. The collagen content in the capsule was quantified using ImageJ software.[29] Two experienced pathologists blinded to the experimental groups independently conducted the analysis.

Immunohistochemical Techniques (IHC)

The tissue sections from the shoulder specimens were dehydrated, washed with purified water, placed in 0.01 M citrate buffer (pH 6.0), and heated in a microwave at medium-high for 2–8 min for antigen retrieval, then closed at room temperature using 3% H_2O_2 for 15–30 min. The antibody was diluted with 5% bovine serum albumin (BSA; Sigma-Aldrich), and rabbit anti-chemokine ligand 2 polyclonal antibody (NBP1-07035, Novus Biologicals, 1:500) was added as primary antibody overnight at 4°C followed by HRP-labeled goat anti-rabbit IgG antibody (AS1107, Aspen Biotechnology, 1:200), incubated at 37°C for 30 min, and washed with PBS. DAB solution was added for color

development under a microscope and stained with hematoxylin (Sigma-Aldrich). The samples were observed using a white-light microscope (CX31, Olympus, Tokyo, Japan) with three randomly selected fields per section. The percentage of CCL2 positive area in the synovium was calculated using ImageJ software, with the mean as the final result.[30]

Immunofluorescent Staining (IF)

The tissue sections from the shoulder specimens were deparaffinized and underwent antigen retrieval as described. The antibody was diluted with 5% BSA, and sections were treated with primary antibody working solution, then incubated overnight at 4°C (Primary antibodies: mouse anti-CD68 monoclonal antibody, ab955, abcam, 1:50; rabbit anti-iNOS polyclonal antibody, ab283655, abcam, 1:50; rabbit anti-mannose receptor monoclonal antibody, ab300621, abcam, 1:200; mouse anti-smooth muscle actin (α-SMA) monoclonal antibody, Sc-53142, Santa Cruz, 1:50). After re-warming and PBS washing, the sections were treated with secondary antibody solution (CY3 Coupled Goat Anti-Rabbit IgG Antibody, GB21303, Servicebio, 1:100; CoraLite488 Coupled Goat Anti-Mouse IgG Antibody, SA00013-1, Proteintech, 1:100; CY3 Coupled Goat Anti-Mouse IgG Antibody, AS1111, Aspen Biotechnology, 1:100). Sections were incubated at 37°C for 40 min protected from light, washed with PBS, and stained with DAPI (D8417-1MG, Sigma-Aldrich) for 20–30 min at room temperature. After PBS washing, sections were sealed with anti-fluorescence quenching sealer and observed using an upright fluorescence microscope (Eclipse Ci-L, Nikon, Tokyo, Japan). Three random fields per section were selected to count $CD68^+$ $iNOS^+$, $CD68^+$ $CD206^+$, and $\alpha\text{-}SMA^+$ cells using ImageJ software and the average was taken as the final result.[31] The co-localized fluorescence intensity was also analyzed.[32]

Protein 3D Structure Modeling and Protein-Protein Interaction Prediction

The corresponding amino acid sequences were uploaded to the AlphaFold Protein Structure Database for modeling.[33] CCL2, iNOS, and α-SMA sequences were obtained from UniProt database (ID: P14844, Q06518, and P62738), while the CD206 sequence was obtained from NCBI database (ID: 291327). Protein interactions between CCL2 and iNOS, CCL2 and CD206, and CCL2 and α-SMA were analyzed using HDOCK server, where a docking score below −200 indicated possible binding, with lower values showing stronger affinity; a confidence score above 0.8 indicated predictions close to the real structure, with accuracy increasing as values approached 1.[34] The protein structure file with the highest score was imported into PyMol 2.3.0 software (Schrödinger LLC, New York, USA) for visualization.

Statistical Analysis

All statistical analyses were performed using Prism 10.1.2 software (GraphPad Software, LLC, California, USA). Unless otherwise specified, differences between multiple groups were analyzed using one-way or two-way ANOVA, followed by Tukey's post hoc test for pairwise comparisons. All data are presented as mean ± SD. Statistical significance was set at $p < 0.05$.

Results

Effective Improvement of Shoulder Function and Mobility in FS Rats by Acupotomy

To evaluate the effectiveness of acupotomy in reducing shoulder inflammation, improving joint endurance, and enhancing mobility in FS rats, we conducted a comprehensive analysis using joint inflammation scoring, gait analysis, and measurements of the maximum passive abduction angle. After modeling, all groups except the Control exhibited significant redness and swelling, petechiae on the left forelimbs, and joint contracture, with arthritis scores indicating heightened inflammation. Shoulder inflammation in acupotomy-treated rats was significantly reduced compared to that in the Untreated group, while the Sham Apo group still exhibited pronounced inflammation, both in appearance and score (Figure 2A and B). Gait analysis showed that the left forepaw landing area increased from 0.719 cm^2 to 1.477 cm^2 post-treatment, with reduced disparity with the right forepaw, indicating the benefit of acupotomy on joint endurance (Figure 2C and D). The mean maximum passive abduction angle in the Acupotomy group reached 150.76°, showing a 22.39% increase over the Untreated group's 123.2°, while Sham Apo showed no therapeutic effect (Figure 2E and F). These results demonstrated the effectiveness of acupotomy in alleviating FS symptoms and improving shoulder function.

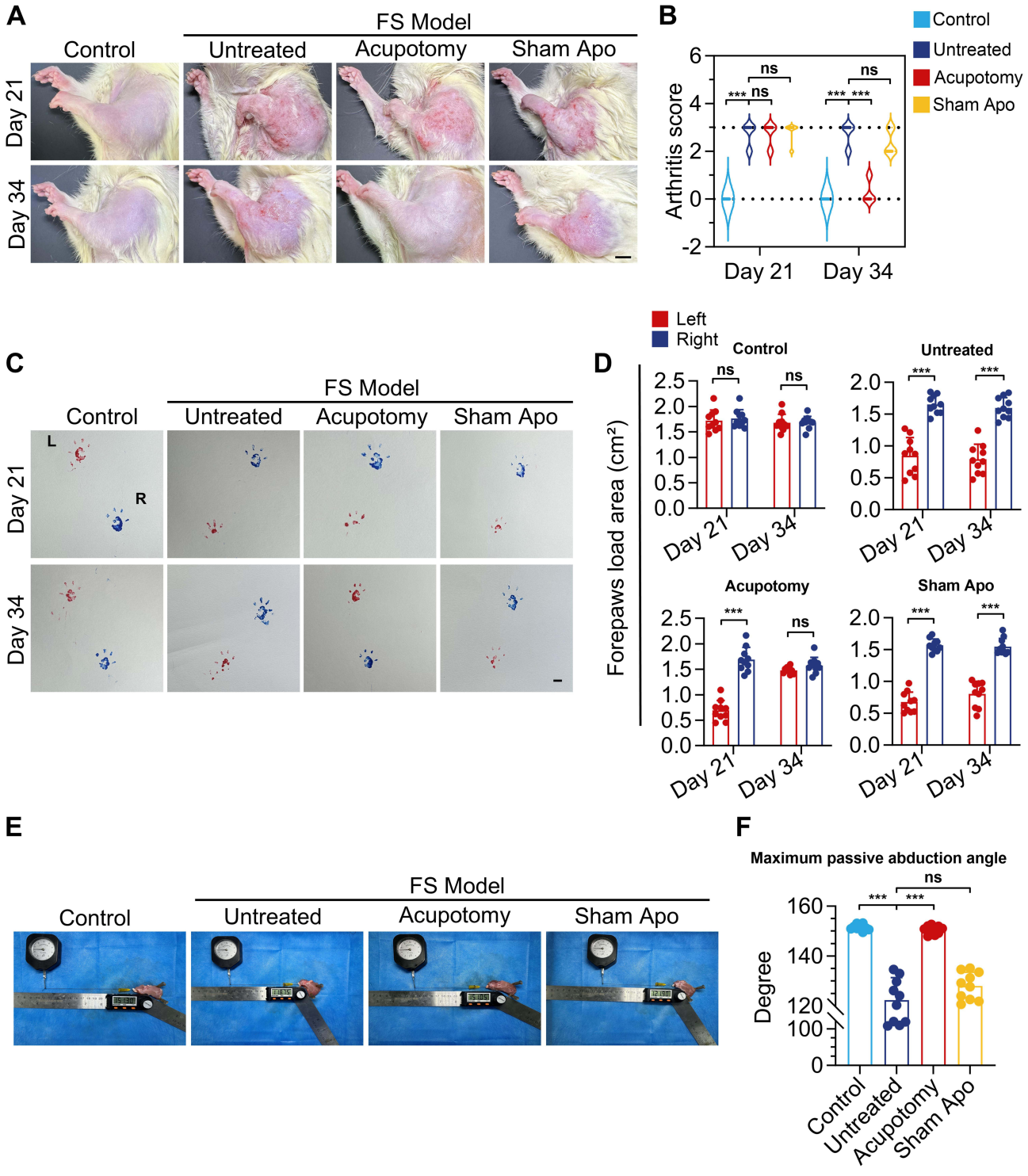

Figure 2 Effective improvement of shoulder function and mobility in FS rats by acupotomy. (**A**) Representative images of the left forelimbs on days 21 and 34. scale bar = 1 cm. (**B**) Statistical analysis of the left compromised shoulder arthritis scores on days 21 and 34 (n = 10). (**C**) Representative images of the left (red) and right (blue) forepaws gait analysis inkblot maps on days 21 and 34. scale bar = 1 cm. (**D**) Statistical analysis of left and right forepaws landing areas on days 21 and 34 (n = 10). (**E**) Representative images of the maximum passive abduction angle measurements of the glenohumeral joint. (**F**) Statistical analysis of the maximum passive abduction angle (n = 10). Data are presented as the mean ± SD. ***p < 0.001.

Abbreviations: ns, no significance; L, left forepaw; R, right forepaw; FS, frozen shoulder; Sham Apo, sham acupotomy.

https://doi.org/10.2147/JIR.S550202

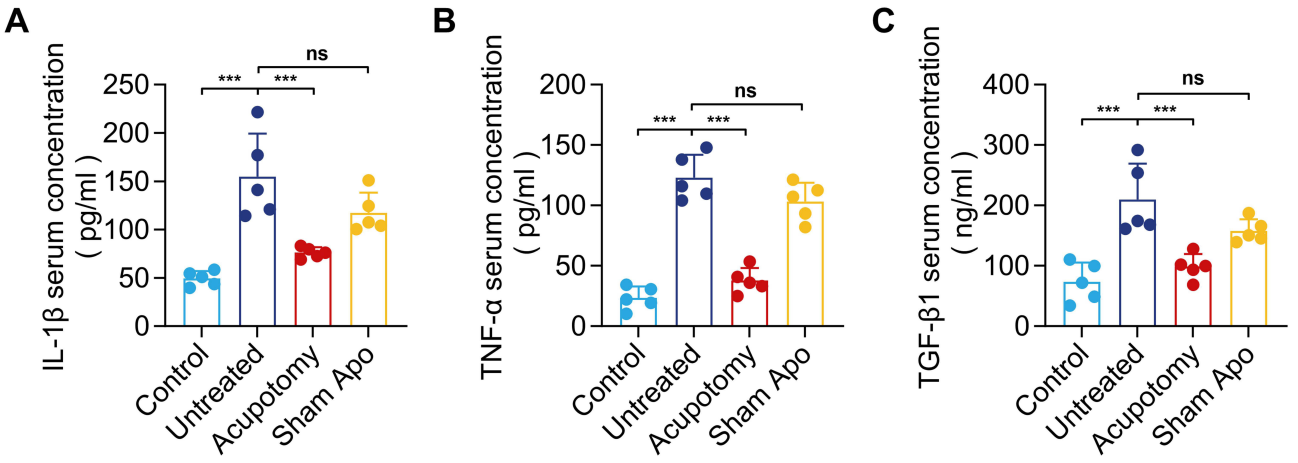

Figure 3 Acupotomy significantly reduced serum levels of (**A**) IL-1β, (**B**) TNF-α, and (**C**) TGF-β1 (n = 5). Data are presented as the mean ± SD. ***p < 0.001.
Abbreviations: ns, no significance; IL-1β, interleukin-1 beta; TNF-α, tumor necrosis factor-alpha; TGF-β1, transforming growth factor-beta 1; Sham Apo, sham acupotomy.

Acupotomy Effectively Reduced Serum IL-1β, TNF-α, and TGF-β1 Levels

To evaluate the alterations in serum concentrations of inflammatory and fibrotic markers following acupotomy, we quantified the serum levels of IL-1β, TNF-α, and TGF-β1 utilizing ELISA. The findings indicated a significant reduction in the serum levels of IL-1β, TNF-α, and TGF-β1 post-acupotomy compared to the Untreated group (Figure 3A–C). These results suggested that the therapeutic efficacy of acupotomy in FS may result from the reduced release of pro-inflammatory and pro-fibrotic mediators.

Acupotomy Alleviated Inflammatory Infiltration in the Capsule and Reduced the Fibrotic Regions Therein

To assess histological alterations after acupotomy, H&E and Masson's trichrome staining were performed on tissue sections. Examination revealed substantial inflammatory cell aggregates within the capsules of the Untreated and Sham Apo groups, with indistinct synovial margins and significant thickening. After acupotomy, inflammatory infiltration improved markedly, with an even-surfaced synovial edge and normalized synovial thickness (Figure 4A). The treated fibrous layer showed organized alignment and reduced collagen deposition compared with the pathological features observed in the other groups (Figure 4B). Semiquantitative scores indicated that acupotomy significantly ameliorated the number of synovial lining layers, resident cell density, and inflammatory infiltrate versus the Untreated group (Figure 4C–E), and reduced the fibrotic area by approximately 37.68% (Figure 4F). Overall, acupotomy effectively reversed the capsular pathological changes associated with inflammation and fibrosis in FS rats.

Acupotomy Downregulated the Transcript Levels of Pro-Inflammatory and Pro-Fibrotic Related Genes within the Capsule

To confirm the hypothesis that acupotomy ameliorates fibrosis by modulating capsular inflammation, we investigated the differential expression of inflammation- and fibrosis-associated factors in capsule tissues utilizing RT-qPCR. The findings indicated significant variations in gene expression among the four groups (Figure 5A). Notably, the expression levels of the inflammatory cytokines *Il1b, Tnfα*, and *Ifng*, along with the fibrosis-related factors *Tgfβ1, Smad3*, and *Col1a1*, were synergistically reduced in the capsules subjected to acupotomy treatment, with levels significantly lower than those observed in the Untreated group. Conversely, this phenomenon was not evident in the Sham Apo group (Figure 5B–G). These results implied that acupotomy could mitigate FS fibrosis by reducing inflammation within the capsule.

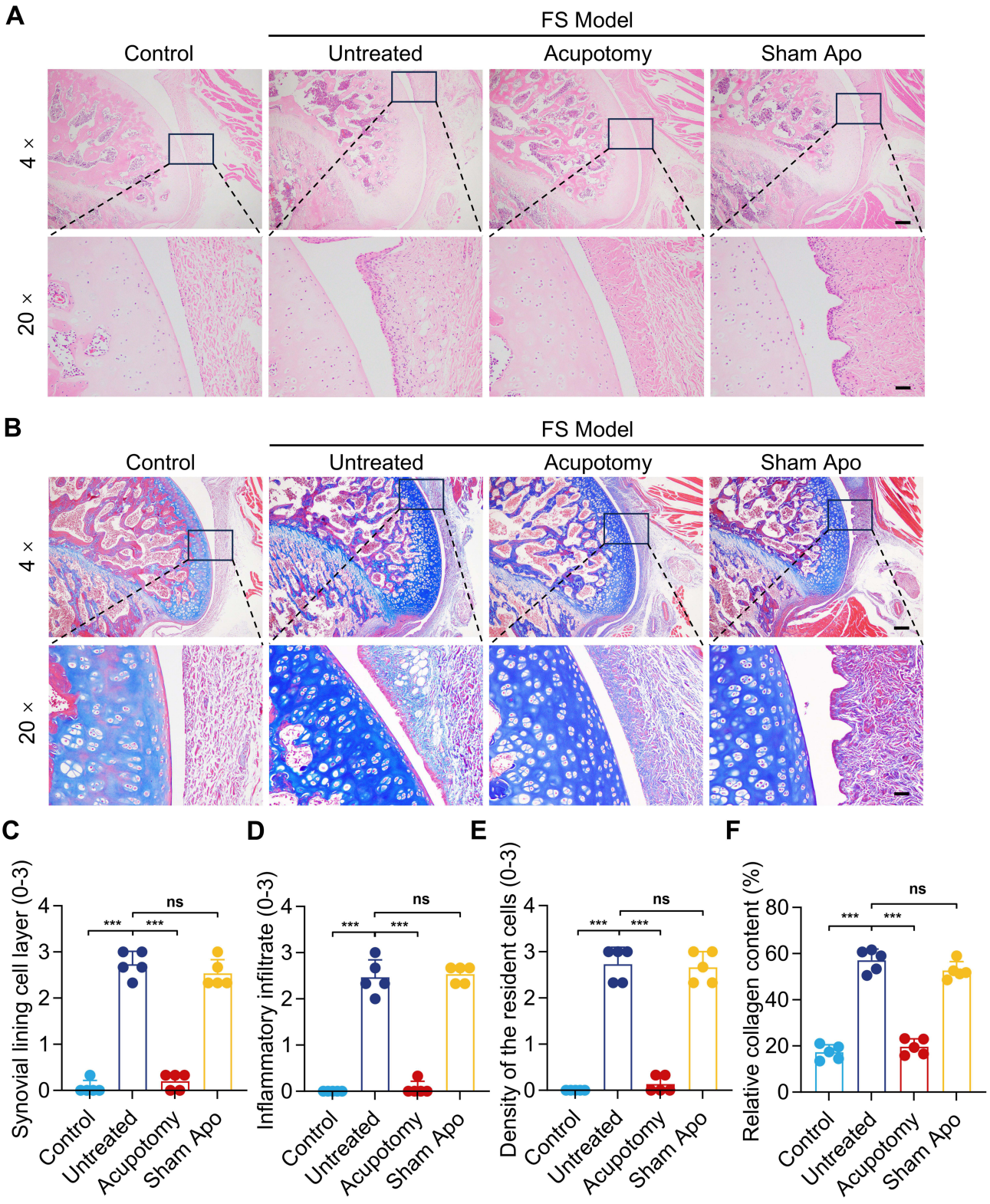

Figure 4 Acupotomy alleviated inflammatory infiltration in the capsule and reduced the fibrotic regions therein. (**A**) Representative images at 4 × and 20 × magnifications of H&E staining. (**B**) Masson's trichrome staining of representative images at 4 × and 20 × magnifications. The capsular (**C**) synovial lining cell layer number, (**D**) inflammatory infiltrate, (**E**) resident cell density, and (**F**) relative collagen content were assessed histologically using a semiquantitative scoring method (n = 5). 4 ×: scale bar = 200 μm; 20 ×: scale bar = 50 μm. Analyses were performed using one-way ANOVA followed by Tukey's multiple comparison test. Data are presented as the mean ± SD. ***p < 0.001.

Abbreviations: ns, no significance; FS, frozen shoulder; sham Apo, sham acupotomy.

https://doi.org/10.2147/JIR.S550202

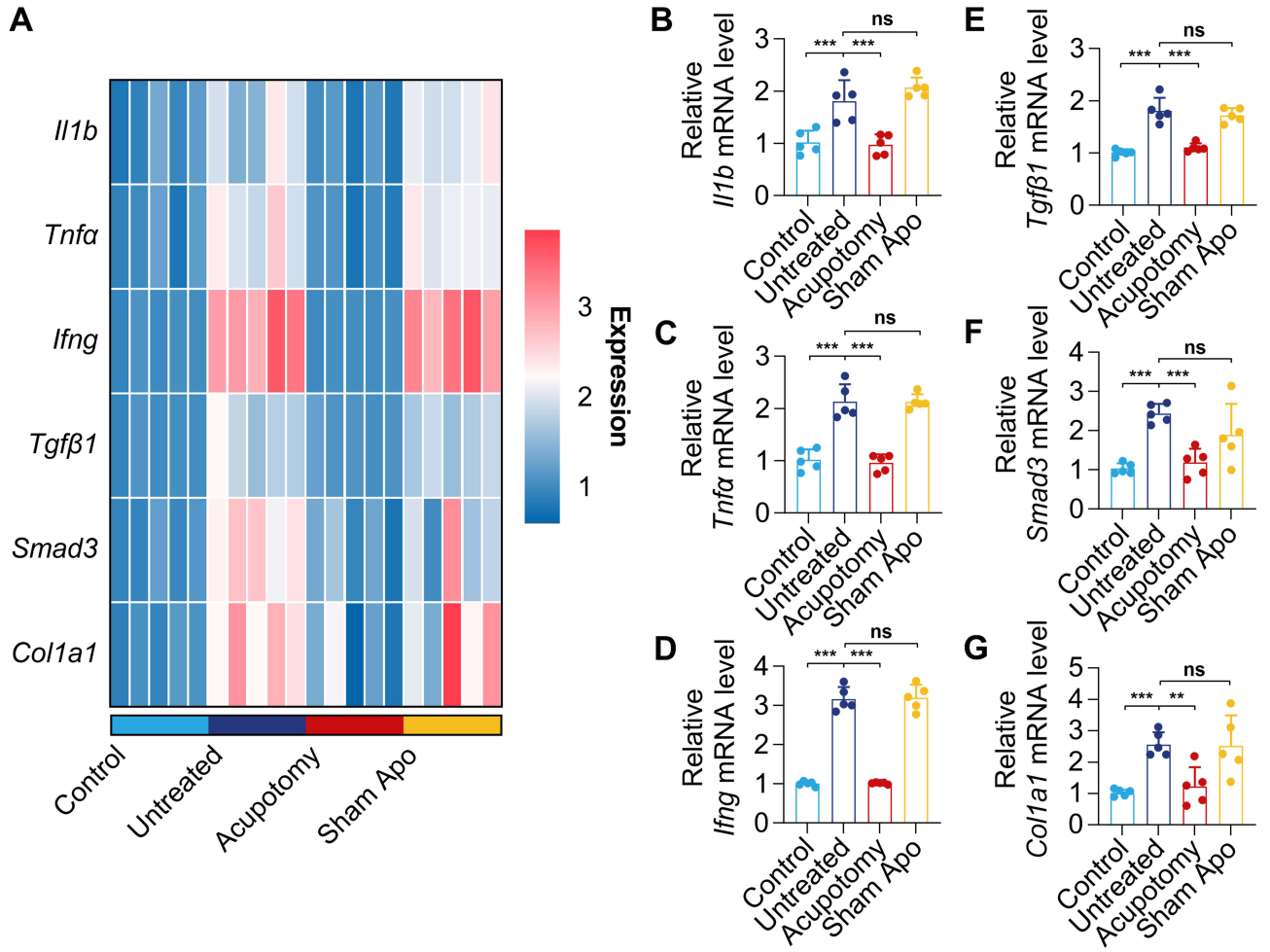

Figure 5 Acupotomy downregulated the transcript levels of pro-inflammatory and pro-fibrotic related genes within the capsule. (**A**) Heatmap of the expression patterns of inflammatory and fibrotic genes in the capsules (n = 5 per group, data are shown for 20 samples in total). Red indicates high expression, blue indicates low expression, and numbers 1–3 represent the degree of gene expression. RT-qPCR assessment of the relative transcript levels of (**B**) *Il1b*, (**C**) *Tnfα*, (**D**) *Ifng*, (**E**) *Tgfβ1*, (**F**) *Smad3*, and (**G**) *Col1a1* in the capsules (n = 5). Gene expression levels were normalized to *Gapdh*. Data are presented as the mean ± SD. **p < 0.01; ***p < 0.001.

Abbreviations: ns, no significance; *Il1b*, interleukin-1 beta; *Tnfα*, tumor necrosis factor-alpha; *Ifng*, interferon gamma; *Tgfβ1*, transforming growth factor-beta 1; *Smad3*, mothers against decapentaplegic homolog 3; *Col1a1*, collagen type I alpha 1 chain; *Gapdh*, glyceraldehyde-3-phosphate dehydrogenase; Sham Apo, sham acupotomy.

Acupotomy Inhibited Macrophage Recruitment and M1/M2 Polarization in the Capsule

In order to investigate the effect of acupotomy on FS progression via modulating macrophages, we characterized macrophages and M1/M2 subpopulations using immunofluorescence detection of CD68 (pan-macrophages), iNOS (M1), and CD206 (M2). The results showed an appreciable increase in the total number of macrophages and fluorescence signals in the Untreated group compared to the Control group, whereas acupotomy considerably reduced macrophage recruitment and fluorescence intensity (Figure 6A and B). Additionally, we identified that the quantities of M1 and M2 macrophages were significantly elevated in the Untreated group compared to the Control group, but were markedly reduced in the Acupotomy group compared to the Untreated group (Figure 6C and D). Analysis further indicated that M2 macrophages were 1.54-fold higher than M1 macrophages in the Untreated group, whereas acupotomy simultaneously reduced M1 and M2 macrophage populations, particularly M2, helping to restore their balance (Figure 6E). Our findings suggested that acupotomy inhibited macrophage recruitment and regulated M1/M2 polarization, shifting the macrophage balance toward homeostasis.

Acupotomy Reduced CCL2 and α-SMA Levels in the Capsule

CCL2, a pivotal chemokine involved in the regulation of macrophage migration, its expression level is directly correlated with the extent of macrophage recruitment in lesions.[35] To further ascertain whether the reduction in macrophage

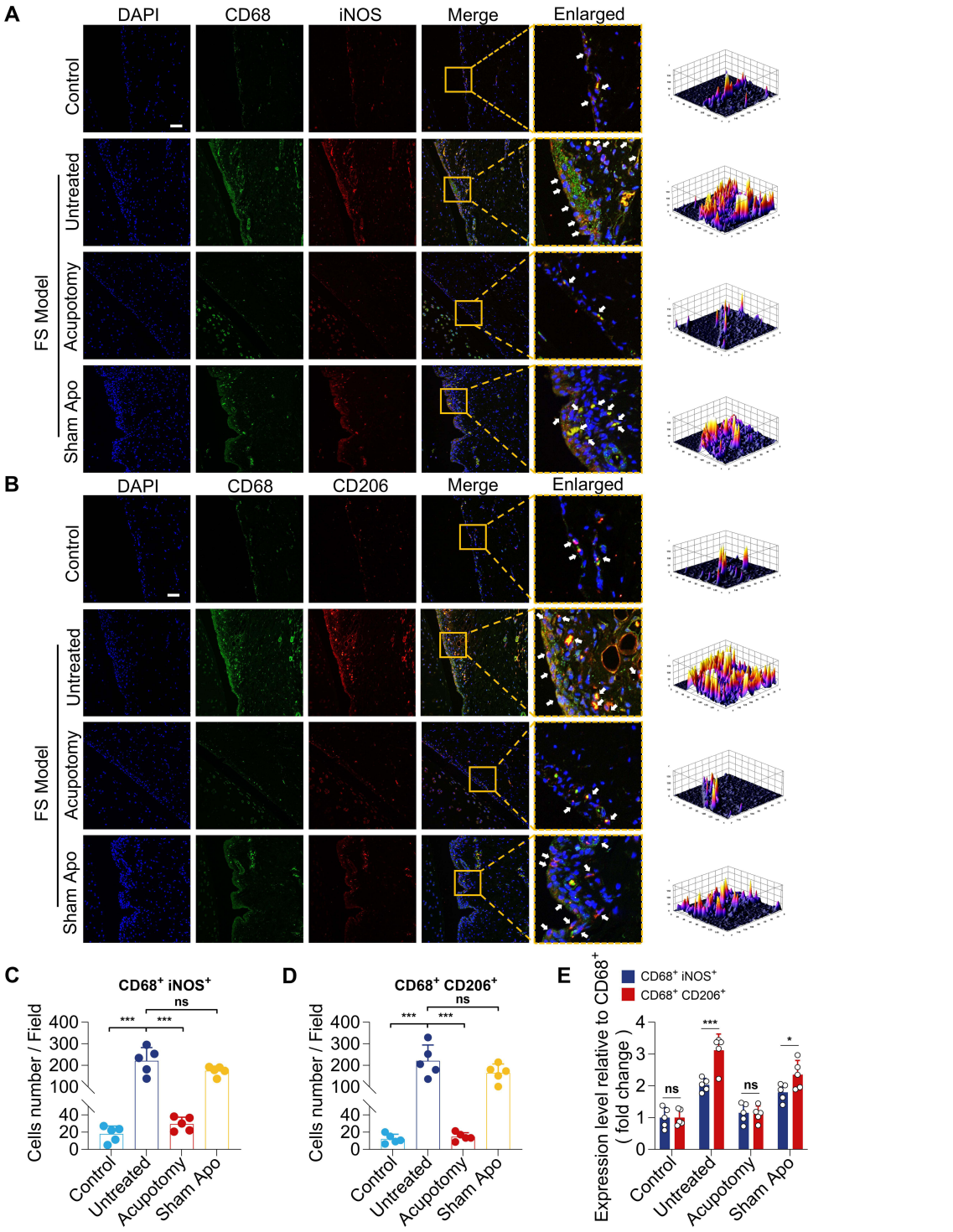

Figure 6 Acupotomy inhibited macrophage recruitment and M1/M2 polarization in the capsule. (**A**) Representative immunofluorescence images of CD68 (green, pan-macrophage marker), iNOS (red, M1 macrophage marker), and DAPI (blue). The right panel presents three-dimensional topographic maps of the co-localized fluorescence intensity. (**B**) Representative immunofluorescence images of CD68 (green, pan-macrophage marker), CD206 (red, M2 macrophage marker), and DAPI (blue). The right panel presents three-dimensional topographic maps of the co-localized fluorescence intensity. Statistical analysis of the numbers of (**C**) CD68+ iNOS + macrophages and (**D**) CD68+ CD206+ macrophages per field (n = 5). (**E**) Statistical analysis of the relative expression comparison between $CD68^+$ $iNOS^+$ macrophages and $CD68^+$ $CD206^+$ macrophages compared to $CD68^+$ macrophages (n = 5). White arrows indicate co-localized macrophages. Scale bar = 50 μm. Data are presented as the mean ± SD. *p < 0.05; ***p < 0.001.

Abbreviations: ns, no significance; CD68, cluster of differentiation 68; iNOS, inducible nitric oxide synthase; CD206, macrophage mannose receptor; FS, frozen shoulder; Sham Apo, sham acupotomy.

https://doi.org/10.2147/JIR.S550202

infiltration observed with acupotomy was associated with CCL2, immunohistochemical staining for CCL2 was performed on sections to evaluate its therapeutic role. Our observations revealed that in both the Untreated group and the Sham Apo group, affected areas exhibiting high CCL2 expression coincided with sites of positive staining of macrophage markers, with a significant overlap in their spatial distribution (Figures 6A, B and 7A). This consistent distribution

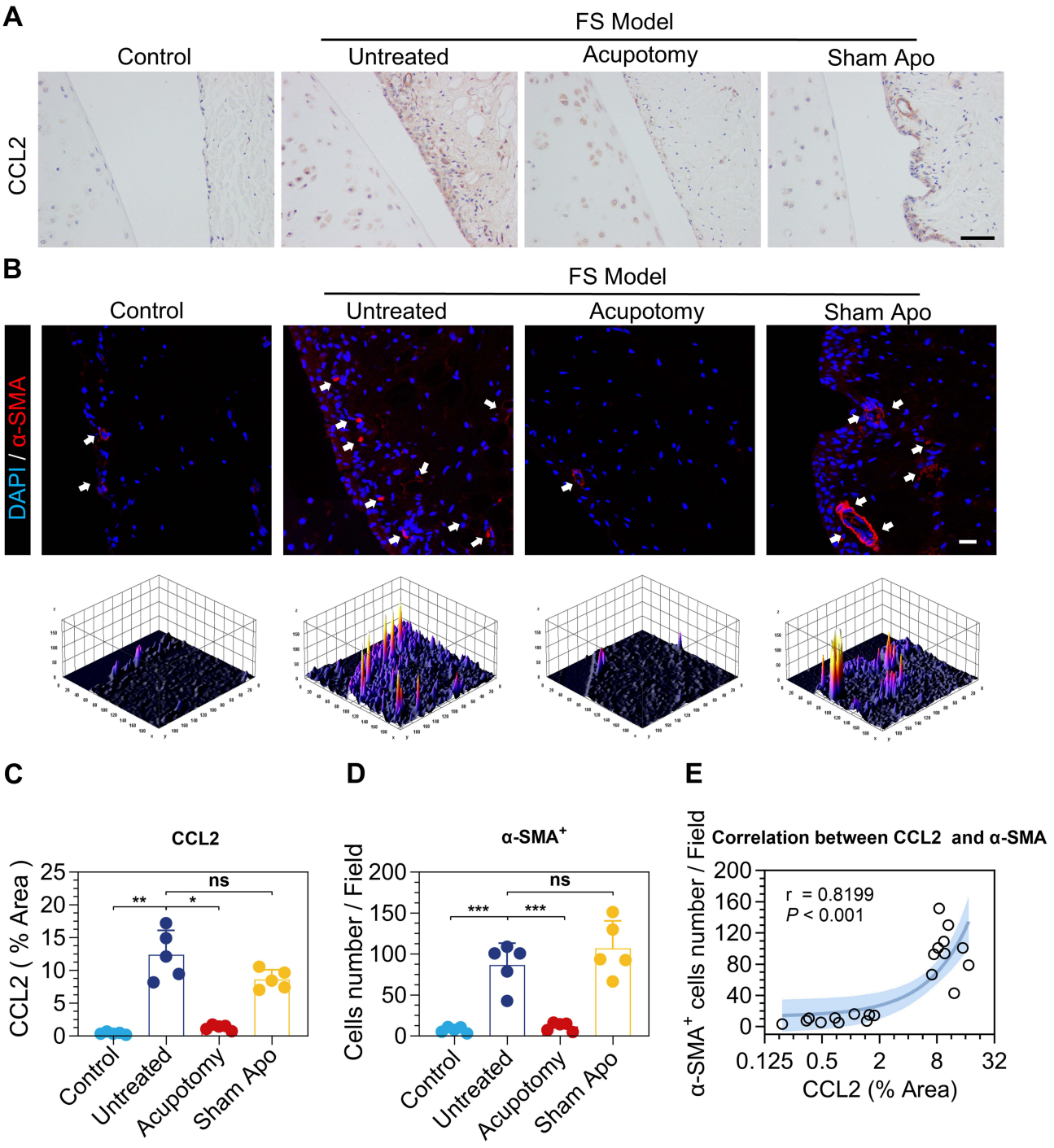

Figure 7 Acupotomy reduced CCL2 and α-SMA levels in the capsule. (**A**) Representative image of immunohistochemical CCL2 staining. scale bar = 50 μm. (**B**) Representative immunofluorescence images of α-SMA (red) and DAPI (blue). scale bar = 20 μm. White arrows indicate α-SMA-positive cells. Three-dimensional topographic maps of the fluorescence intensity are shown below. (**C**) Statistical analysis of CCL2 positive area percentage (n = 5). (**D**) Statistical analysis of α-SMA-positive cells per field of view (n = 5). (**E**) Scatter plot showing the correlation between CCL2 and α-SMA expression (n = 5 per group, data are shown for 20 samples in total). Spearman correlation coefficient (r) assessed correlation strength, with p-values reported for two-tailed tests. Data are presented as the mean ± SD. *p < 0.05; **p < 0.01; ***p < 0.001.
Abbreviations: ns, no significance; CCL2, chemokine (C-C motif) ligand 2; α-SMA, alpha-smooth muscle actin; FS, frozen shoulder; Sham Apo, sham acupotomy.

pattern indicated that CCL2 expression at the lesion site paralleled macrophage infiltration. However, the immunoreactivity of CCL2 within the capsule was markedly reduced following acupotomy therapy (Figure 7A). Representative α-SMA immunofluorescence images from adjacent sections are included to provide morphological comparison (Figure 7B). Furthermore, quantitative analysis based on immunohistochemistry confirmed that the CCL2-positive area decreased by approximately 11.08% in the Acupotomy group compared to the Untreated group (Figure 7C). These findings suggested that acupotomy effectively diminished total macrophage accumulation in the capsule by inhibiting CCL2 expression.

Given that elevated α-SMA expression is an apparent characteristic feature of FS,[36] we further examined its expression to elucidate how acupotomy contributes to the alleviation of capsular fibrosis. Our observations showed that the number of α-SMA-positive cells and fluorescence signals in the Untreated group were significantly higher than those in the Control group. These phenomena were significantly optimized following acupotomy compared with the Untreated group (Figure 7B and D). To clarify how CCL2 mediates the anti-fibrotic effects of acupotomy, we further correlated its expression with α-SMA levels, and we observed a strong positive correlation between α-SMA and CCL2 levels (Figure 7E). These findings suggested that acupotomy suppressed α-SMA to ameliorate FS fibrosis, potentially through CCL2 regulation given their pronounced positive correlation.

CCL2 is a Key Hub for Inducing Macrophage Polarization and Fibrosis

Our observations indicated that CCL2 expression followed a pattern similar to that of iNOS, CD206, and α-SMA within the capsule. With the aim of investigate the impact of CCL2 on macrophage polarization and fibrotic progression, we used 3D modeling to predict their interactions. Analysis revealed that CCL2 residues established four primary contacts with iNOS residues, with hydrogen bonding distances exceeding 3 Å, indicating poor binding affinity (Figure 8A). In contrast, the interactions between CCL2 and CD206 residues involved more contact points than between and iNOS, with an average hydrogen bonding distance of 2.9 Å, suggesting stronger binding stability (Figure 8B). CCL2 residues formed six contacts with α-SMA residues, the highest number observed, demonstrating strong interactions, particularly a 2.1 Å distance between ARG-88 and GLU-102, indicating potentially strong electrostatic forces (Figure 8C). These findings indicated that CCL2 could interact with both iNOS and CD206, with stronger CD206 binding, suggesting that CCL2 may facilitate M1/M2 polarization and enhance M2 macrophage marker progression. CCL2 has a high affinity for α-SMA, demonstrating its potential role in the regulation of fibrosis. In conclusion, CCL2 appears to promote macrophage polarization and fibrosis at the computational simulation level.

Discussion

FS is primarily characterized by inflammation and fibrosis of the glenohumeral capsule. Acupotomy has been identified as an effective therapeutic intervention for FS; however, its precise mechanism of action remains incompletely understood. In this study, we observed that acupotomy not only significantly enhanced shoulder function and mobility, but also reversed the pathological progression of capsular fibrosis by attenuating inflammatory responses. In addition, acupotomy productively modulated macrophage recruitment and suppressed M1/M2 polarization within the capsule, as well as decreased the level of α-SMA, which was closely related to the reduction of CCL2. Therefore, this study demonstrates that acupotomy constitutes an effective therapeutic approach and reveals a novel mechanism for mitigating fibrosis in FS.

The common symptoms of FS are shoulder pain and limited range of motion.[2] Intra-articular steroid injections are a prevalent therapy for FS, demonstrating efficacy in alleviating shoulder pain and enhancing mobility; however, clinical benefits typically become apparent at four weeks post-injection and do not last beyond 26 weeks.[37,38] Although acupuncture serves as a valuable non-pharmacological intervention for alleviating shoulder pain and enhancing mobility in patients with FS, circumventing medication-related adverse effects, its optimal efficacy necessitates prolonged and repeated treatment sessions combined with manual reductions.[39] In light of these shortcomings, we propose acupotomy as a novel alternative approach. Clinical data indicate that a single session of acupotomy can swiftly alleviate pain and enhance shoulder mobility; furthermore, the treatment's efficacy can be maintained for up to three years with a low recurrence rate, underscoring its significant advantages in terms of timeliness and effectiveness.[40] Our study similarly demonstrated that acupotomy rapidly enhanced shoulder function and range of motion. This is evidenced by a significant

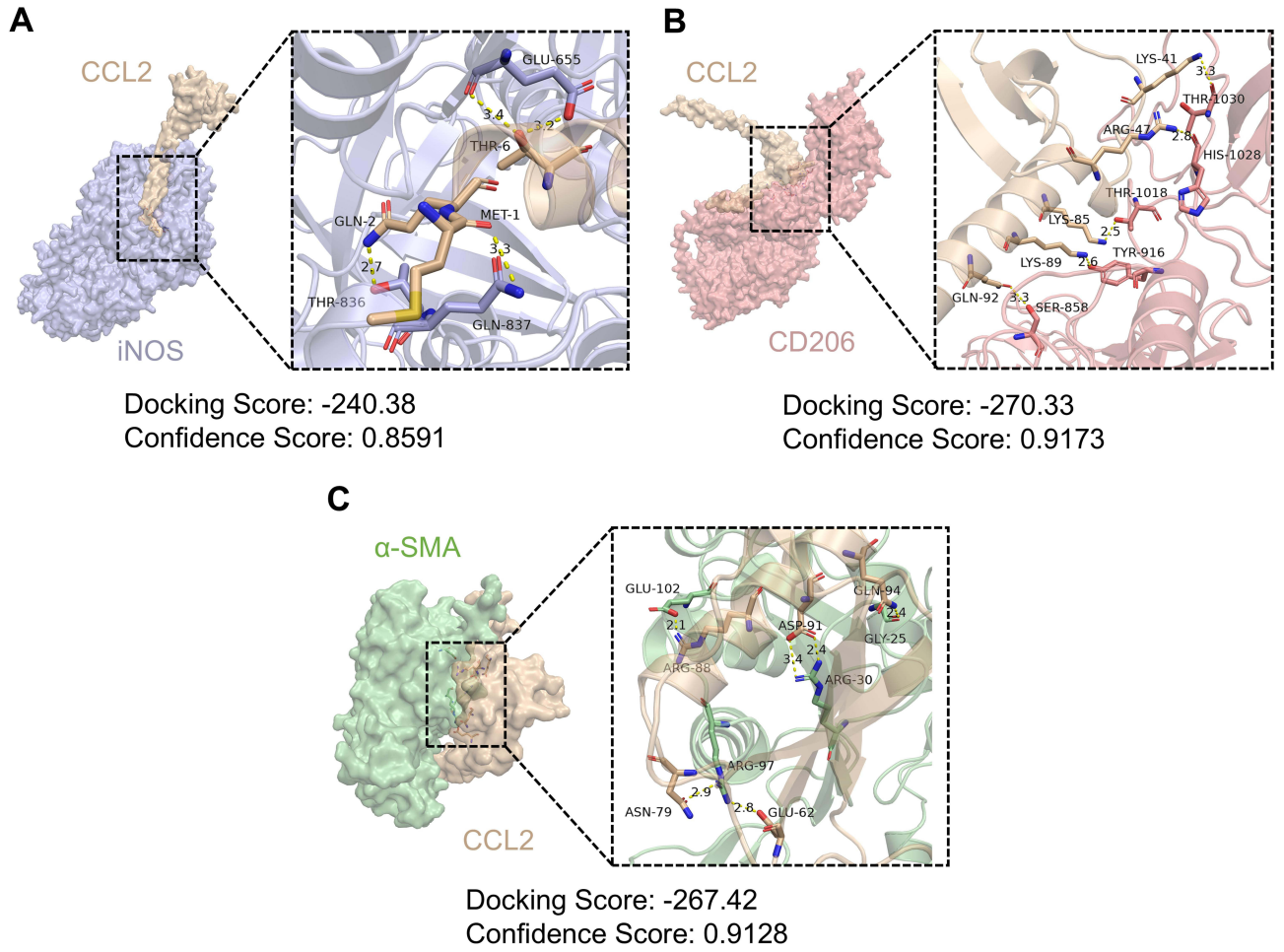

Figure 8 CCL2 is a key hub for inducing macrophage polarization and fibrosis. (**A**) Structural modeling of CCL2-iNOS protein complex illustrates CCL2 in beige and iNOS in blue. The right panel depicts the binding interface, with beige sticks for CCL2 amino acids, blue sticks for iNOS, and yellow dashed lines indicating hydrogen bonds. (**B**) Structural modeling of CCL2-CD206 protein complex, with CCL2 in beige and CD206 in pink. The right panel depicts the binding interface, with beige sticks for CCL2 amino acids, pink sticks for CD206, and yellow dashed lines indicating hydrogen bonds. (**C**) Modeling of CCL2-α-SMA protein complex illustrates CCL2 in beige and α-SMA in green. The right panel depicts the binding interface, with beige sticks for CCL2 amino acids, green sticks for α-SMA, and yellow dashed lines indicating hydrogen bonds. The numbers specify the hydrogen bond lengths. The docking and confidence scores of the composite protein structure models are shown below each figure.
Abbreviations: CCL2, C-C motif chemokine ligand 2; iNOS, inducible nitric oxide synthase; CD206, macrophage mannose receptor; α-SMA, α-smooth muscle actin.

increase in the landing area and passive abduction angle of the affected limb in FS rats following treatment, with observable effects within three days post-treatment. The primary reason for these differences may be attributed to the direct action of acupotomy on intra-articular adhesion sites, which alleviates tissue tension, thereby accelerating shoulder pain relief and enhancing mobility.

Abnormal biomechanical stress drives sustained inflammation and accelerated fibrotic remodeling in FS. Local tension transforms mechanical load into pro-inflammatory signaling, activating inflammation in mechanically sensitive regions and the capsule.[41–43] While biomechanical factors in FS pathogenesis are increasingly recognized, current clinical interventions focus on anti-inflammatory strategies, such as intra-articular corticosteroid injections. Although these treatments provide symptomatic relief, their benefits are often transient, and medications may be restricted by contraindications in certain populations.[44] Phytochemicals such as salvianolic acid B and tetrandrine have demonstrated anti-inflammatory and anti-fibrotic potential in preclinical models. However, their efficacy is limited by nonspecific targeting and potential toxicity.[45,46] More importantly, these strategies do not address the mechanical dysfunctions that perpetuate pathological changes. In contrast, acupotomy may provide a more precise mechanical intervention. As a minimally invasive method, it is helpful in addressing pathological adhesions in areas of concentrated stress, restoring the equilibrium of the local biomechanical microenvironment.[47] Studies have shown that acupotomy can restore joint

biomechanical homeostasis in rabbit models of osteoarthritis by alleviating mechanical stress.[23,48] It concurrently downregulates inflammatory and fibrotic mediators, such as vascular endothelial growth factor (VEGF), IL-1β, and TNF-α, thereby reducing synovial inflammation.[48] Consistent with these findings, our results demonstrated that acupotomy, applied to mechanically overloaded areas, including the coracohumeral ligament, biceps tendon, and rotator cuff complex attachment points,[49] significantly reduced shoulder redness, swelling, and stiffness in rats with FS. Histological analysis revealed reduced capsular inflammation and fibrosis, with decreased expression of multiple pro-inflammatory and pro-fibrotic factors. These results suggest that the therapeutic effects of acupotomy may be linked to its ability to remodel the pathological mechanical microenvironment of FS. However, the precise mechanisms underlying this association remain to be elucidated.

As the primary effector cells in FS-associated fibrosis, fibroblasts within the capsule are activated by persistent inflammation, which upregulates matrix metalloproteinases and collagen genes to drive ECM remodeling.[7,50] Increased expression of α-SMA is a vital indicator of fibroblast activation.[51] A relevant study showed that the rate of α-SMA positivity is highly correlated with the degree of capsular fibrosis.[36] Our results indicated that the number of α-SMA-positive cells in the capsule was significantly decreased after treatment, suggesting that acupotomy may ameliorate fibrosis by restricting the activation of fibroblasts to a certain extent. TGF-β is a powerful pro-fibrotic factor that not only participates in amplifying the inflammatory response, but is also an important mediator of fibroblast activation.[52] It has been substantiated that the TGF-β/Smad3 axis exacerbates fibrosis by upregulating the levels of collagen genes such as *Col1a1 and Col3a1*.[53] Inhibition of signaling in the TGF-β pathway effectively constrains fibroblast activation and facilitates fibrosis regression.[54] This observation aligns with our findings that post-acupotomy, the transcript levels of genes such as *Tgfb1, Smad3*, and *Col1a1* were effectively regulated within the capsule, suggesting that acupotomy might ameliorate FS through a similar pathway; however, the precise molecular mechanisms warrant further investigation.

Macrophages are of significant interest in FS research, especially since their infiltration has been identified in patient capsules.[55] CCL2 is a core regulator that directs the chemotaxis of monocytes/macrophages to participate in tissue inflammation and fibrosis.[56] Previous studies have established CCL2 as a pivotal fibrotic regulator across pulmonary, cardiac, and other organ systems.[57,58] This is contingent upon the capacity of CCL2 to enhance inflammatory infiltration and tissue damage at lesion sites by recruiting macrophages and upregulating pro-fibrotic mediators, such as TGF-β.[17] In our study, we corroborated the pivotal role of CCL2 in modulating the overall macrophage population and fibrosis progression. Furthermore, we demonstrated that acupotomy effectively reduced CCL2 expression, thereby reversing this process, in accordance with the findings of Yoshimura et al.[17] Moreover, our correlation analysis revealed a significant positive correlation between CCL2 and α-SMA expression levels, and protein-protein docking modeling further predicted the binding and interaction modes. Collectively, this evidence identified CCL2 as the pivotal molecular target mediating the anti-fibrotic effects of acupotomy in FS.

Macrophages are phagocytes with high plasticity that can polarize into either classically activated M1 or alternatively activated M2 macrophages, responding to inflammation and tissue repair within a damaged microenvironment.[59] It should be emphasized that M2 macrophages perform several functions, including the secretion of pro-fibrotic factors and promotion of fibroblast activation, and are the drivers of fibrotic lesions.[60] A study demonstrated that M2 macrophages induced in vitro by serum from patients with FS enhanced primary capsule fibroblast activity and promoted ECM deposition via TGF-β/Smad3 pathway, but M1 macrophages did not exhibit these effects, highlighting the critical pathogenic role of M2 macrophages in FS.[61] Recent research has proven that inhibiting M2 polarization of macrophages constitutes an effective strategy for intervening in the fibrotic process. In the context of cardiac fibrosis, the activation of the phosphoinositide 3-kinase gamma (PI3K-γ) pathway prompts myocardial macrophages to differentiate into M2 macrophages, subsequently inducing the secretion of TGF-β1 and initiating atrial fibrosis, the application of the PI3K-γ inhibitor IPI549 can effectively suppress M2 polarization and further block collagen deposition.[62] Luo et al leveraged nanotechnology targeting the endoplasmic reticulum of macrophages, further enabling precise regulation of M2 polarization, thereby alleviating renal fibrosis and enhancing renal function.[63] These studies indicate that inhibiting M2 macrophages appears to be more advantageous for ameliorating fibrotic diseases. Similarly, our findings showed that acupotomy reduced both M1 and M2 macrophages in the capsule, with a more pronounced decrease in M2 macrophages, suggesting that acupotomy not only modulates macrophage polarization, but also offers greater benefits in suppressing

pro-fibrotic macrophage activity. In conjunction with the tendency of acupotomy to downregulate macrophage recruitment, its optimization of macrophage polarization occurs based on a reduction in the overall number of macrophages, as blocking macrophage infiltration indirectly reduces the pool of polarizable macrophages. This polarization optimization may be attributed to the synergistic suppression of inflammation and CCL2 expression. Currently, the relationship between CCL2 and macrophage polarization remains inconclusive. Interestingly, we found that CCL2 interacts with polarization markers through computational simulations, suggesting its potential influence on macrophage polarization. In summary, the inhibition of macrophage recruitment mediated by CCL2 may represent a crucial mechanism by which acupotomy reshapes the immune microenvironment in FS through mechanical release. Nevertheless, this proposed link requires further investigation using CCL2 gene ablation and other targeted interventions.

There are still some limitations in this study. First, we temporarily lack observations on the differences in the therapeutic effects of FS according to acupotomy treatment frequency and duration of action. Second, preliminary findings indicated that the expression of CCL2 and macrophage polarization markers exhibited similar trends and interactions. However, the precise mechanism by which acupotomy influences CCL2 to affect macrophage polarization requires further investigation in subsequent research.

Conclusion

In this study, we verified that acupotomy significantly ameliorated glenohumeral joint dysfunction and histopathological alterations, which were closely related to the reduction of inflammatory and pro-fibrotic factors. This mechanism involved the capacity of acupotomy to inhibit CCL2-mediated macrophage recruitment and to modulate subsequent M1/M2 polarization, thereby decreasing α-SMA expression and capsular fibrosis.

Acknowledgments

In the course of preparing this manuscript, we exclusively employed Paperpal (https://paperpal.editage.cn/) for language refinement and enhancement of readability. We affirm that the tool was not involved in any aspect of the research design, data collection, analysis, or decision-making processes. Graphial abstract Created in BioRender. Liang, H. (2025) https://BioRender.com/zb7bylt.

Funding

This study was supported by the Natural Science Foundation of Hubei Province (No. 2022CFC043).

Disclosure

Hao Liang, Jialin Li, Su Qiu, Jinyuan Guo, and Jianmin Liu report grants from Department of Science and Technology of Hubei Province, during the conduct of the study. The authors report no conflicts of interest in this work.

References

1. Millar NL, Meakins A, Struyf F, et al. Frozen shoulder. *Nat Rev Dis Primers*. 2022;8(1):59. doi:10.1038/s41572-022-00386-2
2. Karbowiak M, Holme T, Mirza M, Siddiqui N. Frozen shoulder. *BMJ*. 2022;377:e068547. doi:10.1136/bmj-2021-068547
3. Challoumas D, Biddle M, McLean M, Millar NL. Comparison of treatments for frozen shoulder: a systematic review and meta-analysis. *JAMA Network Open*. 2020;3(12):e2029581.doi:10.1001/jamanetworkopen.2020.29581
4. Cho CH, Bae KC, Kim DH. Treatment strategy for frozen shoulder. *Clin Orthop Surg*. 2019;11(3):249–257. doi:10.4055/cios.2019.11.3.249
5. Cucchi D, Di Giacomo G, Compagnoni R, et al. A high level of scientific evidence is available to guide treatment of primary shoulder stiffness: the SIAGASCOT consensus. *Knee Surg Sports Traumatol Arthrosc*. 2024;32(1):37–46. doi:10.1002/ksa.12017
6. Akbar M, McLean M, Garcia-Melchor E, et al. Fibroblast activation and inflammation in frozen shoulder. *PLoS One*. 2019;14(4):e0215301. doi:10.1371/journal.pone.0215301
7. Nishimoto H, Fukuta S, Fukui N, Sairyo K, Yamaguchi T. Characteristics of gene expression in frozen shoulder. *BMC Musculoskelet Disord*. 2022;23(1):811. doi:10.1186/s12891-022-05762-3
8. Akbar M, Crowe LAN, McLean M, et al. Translational targeting of inflammation and fibrosis in frozen shoulder: molecular dissection of the T cell/IL-17A axis. *Proc Natl Acad Sci U S A*. 2021;118(39). doi:10.1073/pnas.2102715118
9. Yang H, Cheng H, Dai R, Shang L, Zhang X, Wen H. Macrophage polarization in tissue fibrosis. *PeerJ*. 2023;11:e16092. doi:10.7717/peerj.16092
10. Guan F, Wang R, Yi Z, et al. Tissue macrophages: origin, heterogenity, biological functions, diseases and therapeutic targets. *Signal Transduct Target Ther*. 2025;10(1):93. doi:10.1038/s41392-025-02124-y

11. Alanazi FJ, Alruwaili AN, Aldhafeeri NA, et al. Pathological interplay of NF-kappaB and M1 macrophages in chronic inflammatory lung diseases. *Pathol Res Pract*. 2025;269:155903. doi:10.1016/j.prp.2025.155903
12. Gao Q, Zhang X, Makarcyzk MJ, et al. Macrophage phenotypes modulate neoangiogenesis and fibroblast profiles in synovial-like organoid cultures. *Osteoarthritis Cartilage*. 2025;33(5):590–600. doi:10.1016/j.joca.2025.02.777
13. Langston PK, Mathis D. Immunological regulation of skeletal muscle adaptation to exercise. *Cell Metab*. 2024;36(6):1175–1183. doi:10.1016/j.cmet.2024.04.001
14. Zhu S, Liu M, Bennett S, Wang Z, Pfleger KDG, Xu J. The molecular structure and role of CCL2 (MCP-1) and C-C chemokine receptor CCR2 in skeletal biology and diseases. *J Cell Physiol*. 2021;236(10):7211–7222. doi:10.1002/jcp.30375
15. Weiskirchen R, Weiskirchen S, Tacke F. Organ and tissue fibrosis: molecular signals, cellular mechanisms and translational implications. *Mol Aspects Med*. 2019;65:2–15. doi:10.1016/j.mam.2018.06.003
16. Guilliams M, Mildner A, Yona S. Developmental and functional heterogeneity of monocytes. *Immunity*. 2018;49(4):595–613. doi:10.1016/j.immuni.2018.10.005
17. Yoshimura H, Nakagawa Y, Muneta T, Koga H. A CCL2/MCP-1 antagonist attenuates fibrosis of the infrapatellar fat pad in a rat model of arthritis. *BMC Musculoskelet Disord*. 2024;25(1):674. doi:10.1186/s12891-024-07737-y
18. Lee CJ, Luo WT, Tam KW, Huang TW. Comparison of the effects of acupotomy and acupuncture on knee osteoarthritis: a systematic review and meta-analysis. *Complement Ther Clin Pract*. 2023;50:101712. doi:10.1016/j.ctcp.2022.101712
19. Qin X, Sun K, Ao Y, et al. Traditional Chinese medicine for frozen shoulder: an evidence-based guideline. *J Evid Based Med*. 2023;16(2):246–258. doi:10.1111/jebm.12530
20. Guo S, Liu D, Yang Y, Hu Z. Clinical efficacy of small needle knife therapy on stage I-II frozen shoulder. *J Vis Exp*. 2023;(201). doi:10.3791/65904
21. Kim DH, Lee KH, Lho YM, et al. Characterization of a frozen shoulder model using immobilization in rats. *J Orthop Surg Res*. 2016;11(1):160. doi:10.1186/s13018-016-0493-8
22. Ahn Y, Moon YS, Park GY, et al. Efficacy of intra-articular triamcinolone and hyaluronic acid in a frozen shoulder rat model. *Am J Sports Med*. 2023;51(11):2881–2890. doi:10.1177/03635465231188524
23. Li Y, Hou Y, Sun J, et al. Therapeutic effect of acupotomy at Sanheyang for cartilage collagen damage in moderate knee osteoarthritis: a rabbit model. *J Inflamm Res*. 2023;16:2241–2254. doi:10.2147/JIR.S400956
24. Honzawa T, Matsuo K, Hosokawa S, et al. CCR4 plays a pivotal role in Th17 cell recruitment and expansion in a mouse model of rheumatoid arthritis. *Int Immunol*. 2022;34(12):635–642. doi:10.1093/intimm/dxac041
25. Min SS, Han JS, Kim YI, et al. A novel method for convenient assessment of arthritic pain in voluntarily walking rats. *Neurosci Lett*. 2001;308(2):95–98. doi:10.1016/S0304-3940(01)01983-8
26. Lin A, Sun Z, Xu X, et al. Self-cascade uricase/catalase mimics alleviate acute gout. *Nano Lett*. 2022;22(1):508–516. doi:10.1021/acs.nanolett.1c04454
27. Qiao Y, Yang Y, Wang J, et al. Tuina in a frozen shoulder rat model: an efficient and reproducible protocol. *J Vis Exp*. 2023;(197). doi:10.3791/65440
28. Krenn V, Morawietz L, Burmester GR, et al. Synovitis score: discrimination between chronic low-grade and high-grade synovitis. *Histopathology*. 2006;49(4):358–364. doi:10.1111/j.1365-2559.2006.02508.x
29. Chen L, Song J, Chen X, et al. A novel genotype-based clinicopathology classification of arrhythmogenic cardiomyopathy provides novel insights into disease progression. *Eur Heart J*. 2019;40(21):1690–1703. doi:10.1093/eurheartj/ehz172
30. Hsieh SL, Yang SY, Lin CY, et al. MCP-1 controls IL-17-promoted monocyte migration and M1 polarization in osteoarthritis. *Int Immunopharmacol*. 2024;132:112016. doi:10.1016/j.intimp.2024.112016
31. Cho HH, Rhee S, Cho DI, et al. IKKepsilon-deficient macrophages impede cardiac repair after myocardial infarction by enhancing the macrophage-myofibroblast transition. *Exp Mol Med*. 2024;56(9):2052–2064. doi:10.1038/s12276-024-01304-0
32. Yan S, Xue P, Sun Y, Bai T, Shao S, Zeng X. Cupric doping hollow prussian blue nanoplatform for enhanced cholesterol depletion: a promising strategy for breast cancer therapy and metastasis inhibition. *Adv Sci*. 2025;12(3):e2409967. doi:10.1002/advs.202409967
33. Varadi M, Bertoni D, Magana P, et al. AlphaFold protein structure database in 2024: providing structure coverage for over 214 million protein sequences. *Nucleic Acids Res*. 2024;52(D1):D368–D375. doi:10.1093/nar/gkad1011
34. Yan Y, Zhang D, Zhou P, Li B, Huang SY. HDOCK: a web server for protein-protein and protein-DNA/RNA docking based on a hybrid strategy. *Nucleic Acids Res*. 2017;45(W1):W365–W373. doi:10.1093/nar/gkx407
35. Dong Y, Dong Y, Zhu C, et al. Targeting CCL2-CCR2 signaling pathway alleviates macrophage dysfunction in COPD via PI3K-AKT axis. *Cell Commun Signal*. 2024;22(1):364. doi:10.1186/s12964-024-01746-z
36. Hettrich CM, DiCarlo EF, Faryniarz D, Vadasdi KB, Williams R, Hannafin JA. The effect of myofibroblasts and corticosteroid injections in adhesive capsulitis. *J Shoulder Elbow Surg*. 2016;25(8):1274–1279. doi:10.1016/j.jse.2016.01.012
37. Skaliczki G, Kovacs K, Antal I, et al. Arthroscopic capsular release is more effective in pain relief than conservative treatment in patients with frozen shoulder. *BMC Musculoskelet Disord*. 2024;25(1):145. doi:10.1186/s12891-024-07275-7
38. Sun Y, Zhang P, Liu S, et al. Intra-articular steroid injection for frozen shoulder: a systematic review and meta-analysis of randomized controlled trials with trial sequential analysis. *Am J Sports Med*. 2017;45(9):2171–2179. doi:10.1177/0363546516669944
39. Lo MY, Wu CH, Luh JJ, et al. The effect of electroacupuncture merged with rehabilitation for frozen shoulder syndrome: a single-blind randomized sham-acupuncture controlled study. *J Formos Med Assoc*. 2020;119(1 Pt 1):81–88. doi:10.1016/j.jfma.2019.03.012
40. Zhou K, Xie X, Liu J, et al. One-time relieving of frozen shoulder motor dysfunction with pure acupotomy: a case report. *Medicine*. 2023;102(52):e36783. doi:10.1097/MD.0000000000036783
41. Hagiwara Y, Kanazawa K, Ando A, et al. Effects of joint capsular release on range of motion in patients with frozen shoulder. *J Shoulder Elbow Surg*. 2020;29(9):1836–1842. doi:10.1016/j.jse.2020.01.085
42. Jump CM, Duke K, Malik RA, Charalambous CP. Frozen shoulder: a systematic review of cellular, molecular, and metabolic findings. *JBJS Rev*. 2021;9(1):e19.00153. doi:10.2106/JBJS.RVW.19.00153
43. Cambre I, Gaublomme D, Burssens A, et al. Mechanical strain determines the site-specific localization of inflammation and tissue damage in arthritis. *Nat Commun*. 2018;9(1):4613. doi:10.1038/s41467-018-06933-4

44. Rangan A, Brealey SD, Keding A, et al. Management of adults with primary frozen shoulder in secondary care (UK FROST): a multicentre, pragmatic, three-arm, superiority randomised clinical trial. *Lancet*. 2020;396(10256):977–989. doi:10.1016/S0140-6736(20)31965-6
45. Yan Y, Zhou M, Meng K, et al. Salvianolic acid B attenuates inflammation and prevent pathologic fibrosis by inhibiting CD36-mediated activation of the PI3K-Akt signaling pathway in frozen shoulder. *Front Pharmacol*. 2023;14:1230174. doi:10.3389/fphar.2023.1230174
46. Zhao H, Kong L, Shen J, et al. Tetrandrine inhibits the occurrence and development of frozen shoulder by inhibiting inflammation, angiogenesis, and fibrosis. *Biomed Pharmacother*. 2021;140:111700. doi:10.1016/j.biopha.2021.111700
47. Hu J, Tong H, Zhang J, Jiang L. Acupotomy for musculoskeletal pain: exploring therapeutic potential and future directions. *J Pain Res*. 2025;18:3027–3036. doi:10.2147/JPR.S518705
48. Guo Y, Xu Y, He M, et al. Acupotomy Improves synovial hypoxia, synovitis and angiogenesis in KOA rabbits. *J Pain Res*. 2023;16:749–760. doi:10.2147/JPR.S396955
49. Kanbe K, Inoue K, Inoue Y, Chen Q. Inducement of mitogen-activated protein kinases in frozen shoulders. *J Orthop Sci*. 2009;14(1):56–61. doi:10.1007/s00776-008-1295-6
50. Yang R, Tang Y, Hou J, et al. Fibrosis in frozen shoulder: activation of IL-6 through PI3K-Akt signaling pathway in synovial fibroblast. *Mol Immunol*. 2022;150:29–38. doi:10.1016/j.molimm.2022.07.007
51. Antar SA, Ashour NA, Marawan ME, Al-Karmalawy AA. Fibrosis: types, effects, markers, mechanisms for disease progression, and its relation with oxidative stress, immunity, and inflammation. *Int J Mol Sci*. 2023;24(4):4004. doi:10.3390/ijms24044004
52. Lodyga M, Hinz B. TGF-beta1 - A truly transforming growth factor in fibrosis and immunity. *Semin Cell Dev Biol*. 2020;101:123–139. doi:10.1016/j.semcdb.2019.12.010
53. Yang Z, Zhang H, Yin M, et al. TGF-beta1/Smad3 upregulates UCA1 to promote liver fibrosis through DKK1 and miR18a. *J Mol Med*. 2022;100 (10):1465–1478. doi:10.1007/s00109-022-02248-6
54. Ng MTH, Borst R, Gacaferi H, et al. A single cell atlas of frozen shoulder capsule identifies features associated with inflammatory fibrosis resolution. *Nat Commun*. 2024;15(1):1394. doi:10.1038/s41467-024-45341-9
55. Hand GC, Athanasou NA, Matthews T, Carr AJ. The pathology of frozen shoulder. *J Bone Joint Surg Br*. 2007;89(7):928–932. doi:10.1302/0301-620X.89B7.19097
56. Lis-Lopez L, Bauset C, Seco-Cervera M, Cosin-Roger J. Is the macrophage phenotype determinant for fibrosis development? *Biomedicines*. 2021;9 (12):1747. doi:10.3390/biomedicines9121747
57. Puukila S, Lawrence MD, De Pasquale CG, et al. Monocyte chemotactic protein (MCP)-1 (CCL2) and its receptor (CCR2) are elevated in chronic heart failure facilitating lung monocyte infiltration and differentiation which may contribute to lung fibrosis. *Cytokine*. 2023;161:156060. doi:10.1016/j.cyto.2022.156060
58. Shen SC, Xu J, Cheng C, et al. Macrophages promote the transition from myocardial ischemia reperfusion injury to cardiac fibrosis in mice through GMCSF/CCL2/CCR2 and phenotype switching. *Acta Pharmacol Sin*. 2024;45(5):959–974. doi:10.1038/s41401-023-01222-3
59. Zhao J, Andreev I, Silva HM. Resident tissue macrophages: key coordinators of tissue homeostasis beyond immunity. *Sci Immunol*. 2024;9(94): eadd1967. doi:10.1126/sciimmunol.add1967
60. Jiang Y, Cai R, Huang Y, et al. Macrophages in organ fibrosis: from pathogenesis to therapeutic targets. *Cell Death Discov*. 2024;10(1):487. doi:10.1038/s41420-024-02247-1
61. Sun Y, Lin J, Luo Z, Zhang Y, Chen J. The serum from patients with secondary frozen shoulder following rotator cuff repair induces shoulder capsule fibrosis and promotes macrophage polarization and fibroblast activation. *J Inflamm Res*. 2021;14:1055–1068. doi:10.2147/JIR.S304555
62. Wu Y, Zhan S, Chen L, et al. TNFSF14/LIGHT promotes cardiac fibrosis and atrial fibrillation vulnerability via PI3Kgamma/SGK1 pathway-dependent M2 macrophage polarisation. *J Transl Med*. 2023;21(1):544. doi:10.1186/s12967-023-04381-3
63. Luo L, Wang S, Hu Y, et al. Precisely regulating M2 subtype macrophages for renal fibrosis resolution. *ACS Nano*. 2023;17(22):22508–22526. doi:10.1021/acsnano.3c05998